Available online at www.sciencedirect.com
SCIENCE DIRECT
Catalysis Today 93–95 (2004) 95–105
CATALYSIS TODAY
www.elsevier.com/locate/cattod

Methane partial oxidation over Ni/CeO_2–ZrO_2 mixed oxide solid solution catalysts

Sitthiphong Pengpanich [a], Vissanu Meeyoo [b,*], Thirasak Rirksomboon [a]

[a] *Petroleum and Petrochemical College, Chulalongkorn University, Bangkok 10330, Thailand*
[b] *Centre for Advanced Materials and Environmental Research, Mahanakorn University of Technology, Bangkok 10530, Thailand*

Available online 6 July 2004

Abstract

In this study, methane partial oxidation (MPO) to synthesis gas over $Ni/Ce_{1-x}Zr_xO_2$ ($x = 0$, 0.25, and 1.0 with varying Ni loading of 5, 10 and 15 wt.%) was investigated over the temperature range of 400–800 °C. The experimental results showed that the catalysts prepared by impregnation method are more active than those prepared by gel impregnation method because of their higher degrees of metal dispersion and reducibility. Under the reaction conditions, MPO over Ni/CeO_2 and $Ni/Ce_{0.75}Zr_{0.25}O_2$ mixed oxide catalysts were active at temperatures above 550 °C whereas that of Ni/ZrO_2 took place at temperatures above 650 °C. The H_2/CO molar ratio of 2.0 ± 0.05 was obtained. Generally, the CH_4 conversion slightly increased while the CO and H_2 selectivities remained unchanged with increasing Ni loading. The $Ni/Ce_{0.75}Zr_{0.25}O_2$ mixed oxide catalysts were found to resist to coke formation more than the other catalysts due to their high degrees of metal dispersion and surface oxygen mobility. The TPO results indicated that a major source of carbon deposition on these catalysts is due to the methane decomposition. Results also showed that the activity and selectivity of the catalysts can be regained after the regeneration under oxidizing atmosphere.

Keywords: Methane; Partial oxidation; Ni/CeO_2–ZrO_2; Solid solution; Coke

1. Introduction

In recent years, a catalytic partial oxidation of methane to synthesis gas: CO and H_2 has been widely investigated as an attractive alternative process to steam reforming since the reaction is mildly exothermic and can produce H_2/CO ratio of 2 which is suitable for methanol or Fischer–Tropsch synthesis.

Many catalysts containing transition metals (Ni, Cu and Fe) [1–5], noble metals (Ru, Rh, Pt and Pd) [6–12] and metal oxides [13–16] were employed in investigations of methane partial oxidation. Among those, Ni-based catalyst shows an excellent catalytic activity in this reaction when compared to noble metal catalysts due to its low cost [17,18]. However, Ni is deactivated easily by coke formation and/or metal sintering.

Carbon deposition on a supported Ni catalyst mainly comes from methane decomposition and CO disproportionation reaction at high temperature. In general, the deposition of carbon would occur over the metallic sites as well as on the acid sites of the support. Therefore, the studies of highly active and stable catalyst have been focused. Many additives were successive to reduce carbon deposition for Ni/Al_2O_3 such as Li, La, K and Na [19]. The use of Ni on different supports such as CaO, SiO_2 and MgO was also reported [4,20]. It was reported that the use of supports in the presence of basic sites such as MgO resulted in enhancing activities and lower carbon deposition [20]. On the other hand, use of reducibility support could result in further activity and decrease coke formation [12,21,22]. Stagg-Williams et al. [23] reported that a higher degree of reduction of catalyst results in an increase in the number of oxygen vacancies and subsequent to resist to carbon deposition.

Recently, Otsuka et al. [16] has reported that CeO_2 could be able to convert methane to synthesis gas with H_2/CO ratio of 2 and that adding Pt black could promote syngas formation rate. This finding is similar to Ni/CeO_2 reported by Dong et al. [24]. They also proposed mechanism over Ni/CeO_2 that CH_4 dissociates on Ni and the resultant carbon species quickly migrate to the interface of Ni–CeO_2 and then react with lattice oxygen of CeO_2 to form CO. However, ceria still has some disadvantages. Ceria has a poor thermal

* Corresponding author. Tel.: +66 2 988 4039; fax: +66 2 988 4039.
E-mail address: vissanu@mut.ac.th (V. Meeyoo).

0920-5861/$ – see front matter © 2004 Elsevier B.V. All rights reserved.
doi:10.1016/j.cattod.2004.06.079

resistance and stability at high temperatures. Ceria-supported Ni with high Ni loading (13 wt.%) was an active catalyst for methane partial oxidation but rapidly deactivated by carbon deposition [20].

The addition of ZrO_2 to CeO_2 can improve its oxygen storage capacity, redox properties, thermal resistance and better catalytic activity at low temperatures [25–29]. It was demonstrated that CeO_2–ZrO_2 mixed oxides produced synthesis gas with a H_2/CO ratio of 2 and the formation rates of H_2 and CO were increased due to the incorporation of ZrO_2 into CeO_2. The oxygen desorption and reduction by H_2 of $Ce_{1-x}Zr_xO_2$ solid solution with $x = 0.5$ took place at lower temperature as compared with pure ceria. In our early study, we have also found that $Ce_{0.75}Zr_{0.25}O_2$ solid solution exhibited the highest reducibility [30]. On the contrary, it was demonstrated that Ni/CeO_2–ZrO_2 with Ce/Zr ratio of 0.25 or small amount of CeO_2 exhibited high catalytic activity for methane partial oxidation [24,31].

In this study, we report on the activity, selectivity and stability of Ni/$Ce_{0.75}Zr_{0.25}O_2$ catalyst compared with Ni/CeO_2 and Ni/ZrO_2 catalysts for methane partial oxidation to synthesis gas over the temperature range of 400–800 °C at atmospheric pressure.

2. Experimental

2.1. Catalyst preparation

Mixed oxide solid solutions of Ce–Zr metals were prepared as catalyst supports via urea hydrolysis. The Ce–Zr mixed oxide solid solution samples were prepared from $Ce(NO_3)_3{\cdot}6H_2O$ (99.0%, Fluka) and $ZrOCl_2{\cdot}8H_2O$ (99.0%, Fluka). The ratio between the metal salts was altered depending on the desired solid solution concentration: $Ce_{1-x}Zr_xO_2$ in which $x = 0$, 0.25 and 1.0. The synthesis procedure has been reported elsewhere [30].

The catalysts prepared by the incipient wetness impregnation method were designated as IMP. To prepare Ni/$Ce_{1-x}Zr_xO_2$ (IMP) catalysts, Ni (5, 10 and 15 wt.%) was loaded by the incipient wetness impregnation method into the supports using its nitrate salt solution.

The catalysts designated as GEL were prepared by the gel impregnation method. In the case of GEL catalysts, a 5 wt.% Ni was loaded during the gel step. The washed gel was added with nickel nitrate salt solution to obtain a desired loading before drying and calcination. The catalysts were then calcined at 500 °C for 4 h in air.

2.2. Catalyst characterizations

BET surface area was determined by N_2 adsorption at 77 K (a five point Brunauer–Emmett–Teller (BET) method using a Quantachrome Corporation Autosorb). Prior to the analysis, the sample was outgassed to eliminate volatile adsorbents on the surface at 250 °C for 4 h.

H_2 uptake and degree of dispersion were determined by pulse technique using a temperature programmed analyzer (ThermoFinnigan modeled TPDRO 1100). Prior to pulse chemisorption, the sample was reduced in H_2 atmosphere at 500 °C for 1 h. Then the sample was purged with N_2 at 500 °C for 30 min and cooled down to 40 °C. A H_2 pulse (99.99% H_2 with a sample loop volume of 0.4 ml) was injected into the sample at 40 °C.

An X-ray diffractometer (XRD) system (Rigaku) equipped with a RINT 2000 wide-angle goniometer using Cu Kα radiation and a power of 40 kV × 30 mA was used for examination of the crystalline structure. The intensity data were collected at 25 °C over a 2θ range of 20–90° with a scan speed of 5°/min (2θ) and a scan step of 0.02° (2θ). The morphology of carbon deposition on the spent catalysts was observed by transmission electron microscopy (TEM) with a JEOL (JEM-2010) transmission electron microscope operated at 200 kV. The samples were dispersed in absolute ethanol ultrasonically, and the solutions were then dropped on copper grids coated with a lacey carbon film.

H_2 temperature programmed reduction (H_2-TPR) experiments were carried out using a TPR analyzer (ThermoFinnigan modeled TPDRO 1100). The sample was pretreated in N_2 atmosphere at 400 °C for 30 min prior to running the TPR experiment, and then cooled down to room temperature in N_2. A 5% H_2/N_2 gas was used as a reducing gas. The sample temperature was raised at a constant rate of 10 °C min^{-1} from room temperature to 950 °C. The amount of H_2 consumption as a function of temperature was determined from a TCD signal.

CH_4 temperature programmed reduction (CH_4-TPR) experiments were carried out in a quartz micro-reactor in a similar manner to H_2-TPR experiments but using a 2% CH_4/He as a reducing gas. The effluent gas composition as a function of temperature was measured using a mass spectrometer (Balzer Instruments modeled Thermostar GSD 300T).

Temperature programmed oxidation (TPO) carried out in a TPO micro-reactor analyzer coupled with an FID was used to quantify the amount of coke formation in the spent catalysts. Typically, a 40 mg sample was heated from room temperature in flowing 2% O_2/He at a heating rate of 10 °C min^{-1} to 900 °C.

2.3. Catalytic activity tests

Catalytic activity tests for methane partial oxidation were carried out in a packed-bed quartz microreactor (i.d. Ø6 mm). Typically, a 100 mg catalyst sample was packed between the layers of quartz wool. The reactor was placed in an electric furnace equipped with K-type thermocouples. The catalyst bed temperature was monitored and controlled by Shinko temperature controllers. The feed gas mixture containing 4% CH_4, 2% O_2 and balanced with He was used for which a gas hourly space velocity (GHSV) was maintained at 106,000 h^{-1} using Brooks mass flow controllers. Measurements were carried out at various furnace

temperatures adjusted sequentially from 400 to 800 °C with an interval of 50 °C. The coke formations on the catalysts were further studied in the same system as for MPO at 700–800 °C with different conditions (GHSV of 53,000 h^{-1} and CH_4/O_2 ratios of 1.6, 2.0 and 2.5).

The gaseous products were chromatographically analyzed using a Shimadzu GC 8A fitted with a TCD. A CTR I (Alltech) packed column was used to separate all products at 50 °C except for H_2O which was trapped out prior to entering the column. The CH_4 conversion (X_{CH_4}), O_2 consumption (X_{O_2}) and selectivity (S) reported in this work were calculated as follows:

$$\%X_{CH_4} = \frac{CH_4^{in} - CH_4^{out}}{CH_4^{in}} \times 100 \quad (1)$$

$$\%X_{O_2} = \frac{O_2^{in} - O_2^{out}}{O_2^{in}} \times 100 \quad (2)$$

$$\%S_{CO} = \frac{CO^{out}}{CO^{out} + CO_2^{out}} \times 100 \quad (3)$$

$$\%S_{H_2} = \frac{H_2^{out}}{H_2^{out} + H_2O^{out}} \times 100 \quad (4)$$

3. Results and discussion

3.1. BET surface area, H_2 uptake and metal dispersion

The BET surface areas, H_2 uptake and metallic Ni dispersion of the catalysts are shown in Table 1. The surface areas of the catalysts are in the range of 80–138 m^2/g. For IMP catalysts, the surface areas were found to decrease with increasing Ni loading. When Ni loading was increased from 5 to 15 wt.%, Ni/CeO_2 (IMP) surface areas were drastically decreased by about 40%. On the other hand, the surface areas of $Ni/Ce_{0.75}Zr_{0.25}O_2$ (IMP) and Ni/ZrO_2 (IMP) catalysts were somewhat decreased by 17 and 8%, respectively.

Table 1
BET surface area, H_2 uptake and dispersion degree of the catalysts

Catalyst	BET surface area (m^2/g)	H_2 uptake ($\mu mol/g$)	Dispersion (%)
5% Ni/CeO_2 (IMP)	135	34.83	8.20
5% $Ni/Ce_{0.75}Zr_{0.25}O_2$ (IMP)	112	39.74	9.33
5% Ni/ZrO_2 (IMP)	138	4.12	0.97
10% Ni/CeO_2 (IMP)	114	33.66	3.95
10% $Ni/Ce_{0.75}Zr_{0.25}O_2$ (IMP)	95	31.04	3.64
10% Ni/ZrO_2 (IMP)	128	3.88	0.46
15% Ni/CeO_2 (IMP)	65	33.61	2.60
15% $Ni/Ce_{0.75}Zr_{0.25}O_2$ (IMP)	93	31.61	2.50
15% Ni/ZrO_2 (IMP)	127	3.47	0.27
5% Ni/CeO_2 (GEL)	128	19.95	4.69
5% $Ni/Ce_{0.75}Zr_{0.25}O_2$ (GEL)	104	6.17	1.45
5% Ni/ZrO_2 (GEL)	124	1.28	0.30

This might be due to the fact that nickel acts as a nucleating agent promoting the sintering and ceria, itself, has low thermal stability [17]. The surface areas of GEL catalysts are barely different from those of IMP catalysts.

The degree of dispersion of Ni/CeO_2 and $Ni/Ce_{0.75}Zr_{0.25}O_2$ catalysts are higher than those of Ni/ZrO_2 catalysts indicating that Ni particles are better dispersed on CeO_2 and $Ce_{0.75}Zr_{0.25}O_2$ than ZrO_2. The dispersion degree was found to decrease as an increase in metal loading. This is due to the formation of NiO bulk particles. It should be noted that the amount of H_2 uptake for the GEL catalysts is lower than that for IMP catalysts indicating a lower exposed Ni metal due to particle encapsulation [32].

3.2. XRD analysis

The structure of the catalysts was determined using an XRD as shown in Fig. 1. For 5% Ni loading catalysts, the XRD patterns of Ni/CeO_2 and $Ni/Ce_{0.75}Zr_{0.25}O_2$ prepared via both IMP and GEL methods exhibited a cubic fluorite structure while the XRD patterns of both the IMP and GEL Ni/ZrO_2 catalysts showed a tetragonal structure. No separate Ni and NiO phases were found by XRD for such a low Ni loading (5 wt.% Ni). This might be postulated that the Ni metal loading is too small to be detected by the XRD. At higher Ni loadings (10 and 15 wt.% Ni), three new peaks at about 37°, 43° and 62° (2θ) indicating a NiO phase were observed. The peak intensity was obviously stronger with increasing Ni loading suggesting that at a low Ni content, NiO was present in the form of nanoparticles while at a high Ni content, bulk NiO agglomerated particles were present [18]. This result appears to be in good agreement with the degree of metal dispersion data.

3.3. H_2-TPR

The H_2-TPR profiles of the IMP catalysts are shown in Fig. 2. For the Ni/CeO_2 (IMP) catalysts, a strong peak with the maximum temperature at ca. 360 °C and another broad peak with the maximum temperature at ca. 800 °C were observed. The first peak was attributed to the reduction of NiO (indicated by XRD analysis) to Ni^0 and the other peak was related to the bulk reduction of CeO_2 from Ce^{+4} to Ce^{+3} [17,31]. An increase in Ni loading does not affect the reduction temperature of NiO over CeO_2 but a small peak with the maximum temperature at ca. 250 °C was observed for the 10 and 15 wt.% Ni loadings. This peak might be due to the reduction of free NiO particles [29] or hydrogen spillover effect [31]. Similar results were found in the case of $Ni/Ce_{0.75}Zr_{0.25}O_2$ (IMP) catalysts which exhibit two peaks with the maxima at ca. 360 and 800 °C. However, a small peak at ca. 250 °C was smaller than that of Ni/CeO_2 indicating a lower amount of free NiO particles. This suggests that NiO–support interactions for $Ni/Ce_{0.75}Zr_{0.25}O_2$ (IMP) catalysts be stronger than those

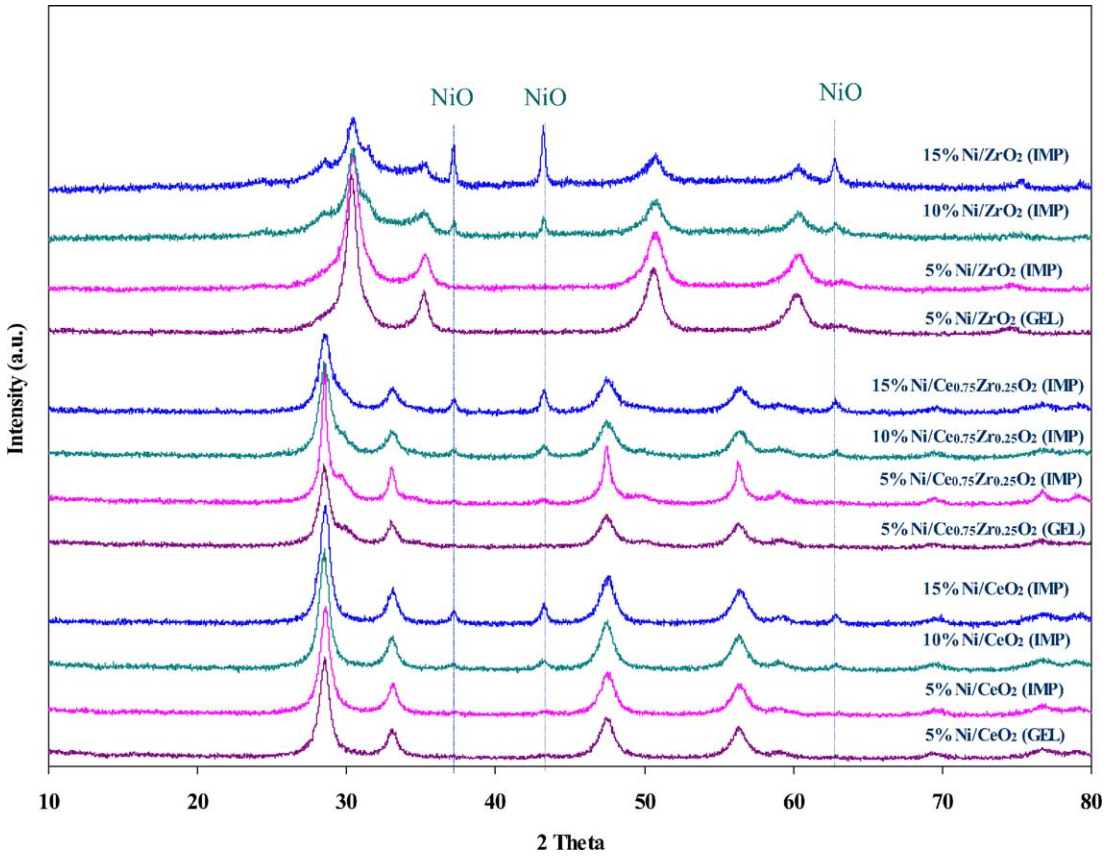

Fig. 1. XRD patterns of Ni over CeO_2, $Ce_{0.75}Zr_{0.25}O_2$ and ZrO_2 catalysts prepared via impregnation and during gel impregnation method calcined at 500 °C.

for Ni/CeO_2 (IMP) catalysts. For the 5 wt.% Ni/ZrO_2 (IMP) catalyst, a peak at temperature ca. 480 °C was observed while no reduction of ZrO_2 was observed (Fig. 2). As an increase in Ni loading (10 and 15 wt.%), the unresolved peak with the maximum temperature at ca. 350 °C was observed. This suggests that there be two kinds of NiO species. The peak at a lower temperature is assigned to a free NiO species interacting weakly with support, and the other peak at a higher temperature is attributed to a complex NiO species interacting strongly with support [29].

The H_2-TPR profiles for the GEL catalysts are similar to those for the IMP catalysts as shown in Fig. 3. However, the reduction profile of 5% $Ni/Ce_{0.75}Zr_{0.25}O_2$ (GEL) is slightly different from that of the IMP catalyst. The catalysts prepared by gel impregnation show a broader reduction peak than those prepared by incipient wetness impregnation. The wideness of peak is due to a broad particle size distribution. Also the GEL reduction temperature is relatively higher than the IMP one. Interestingly, the reduced NiO region of 5% $Ni/Ce_{0.75}Zr_{0.25}O_2$ (GEL) was shifted from the maximum at ca. 350 to 420 °C when compared with that of 5% $Ni/Ce_{0.75}Zr_{0.25}O_2$ (IMP) catalyst. This result indicates that the catalyst prepared by gel impregnation has a higher interaction between NiO and support [17].

3.4. Catalytic activity for methane partial oxidation (MPO)

The catalytic activity for MPO to synthesis gas was tested in a dilute mixture (4% CH_4 and 2% O_2 balanced with He) in the temperature range of 400–800 °C. The supports (CeO_2, $Ce_{0.75}Zr_{0.25}O_2$ and ZrO_2) are not relatively active for MPO as seen in Fig. 4. Dominant MPO products (CO and H_2) were observed at temperatures higher than 600 °C with only about 5% CO yield at 700 °C.

The addition of Ni onto the supports resulted in an increase in MPO catalytic activity. Fig. 4 shows the CH_4 conversion, CO selectivity and H_2 selectivity as functions of temperature for MPO over the IMP and GEL catalysts. For the 5 wt.% IMP catalysts, CH_4 conversion with the complete oxidation products, CO_2 and H_2O, was observed at temperatures < 550 °C for Ni/CeO_2 and $Ni/Ce_{0.75}Zr_{0.25}O_2$ catalysts and at temperatures < 650 °C for Ni/ZrO_2 catalyst. Beyond such temperatures, the CH_4 conversion dramatically increased resulting from the methane partial oxidation reaction. The oxygen was completely consumed and the H_2/CO molar ratio of ca. 2.0 ± 0.05 was obtained at these conditions. The results are similar to that observed by Shishido et al. [32] suggesting that the first stage is corresponding to the combustion of methane followed by steam and CO_2 reforming reactions of methane to synthesis gas.

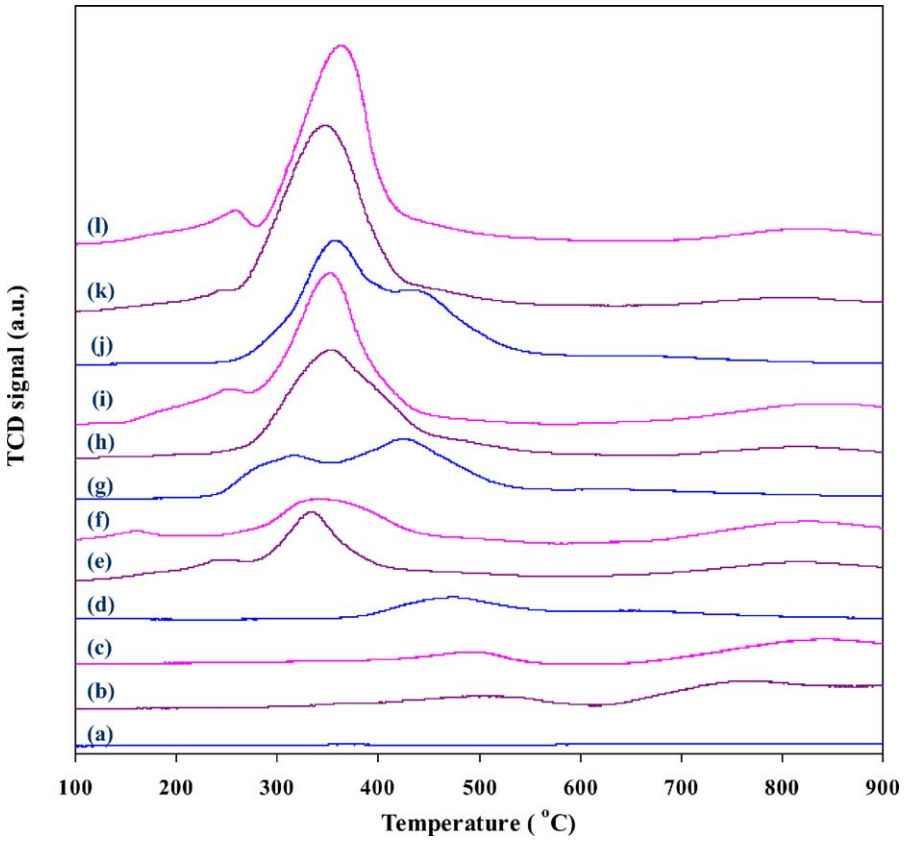

Fig. 2. H_2-TPR profiles of catalysts calcined at 500 °C with a heating rate of 10 °C min^{-1}, a reducing gas containing 5% hydrogen in nitrogen with a flow rate of 30 ml min^{-1}: (a) ZrO_2, (b) $Ce_{0.75}Zr_{0.25}O_2$, (c) CeO_2, (d) 5 wt.% Ni/ZrO_2 (IMP), (e) 5 wt.% $Ni/Ce_{0.75}Zr_{0.25}O_2$ (IMP), (f) 5 wt.% Ni/CeO_2 (IMP), (g) 10 wt.% Ni/ZrO_2 (IMP), (h) 10 wt.% $Ni/Ce_{0.75}Zr_{0.25}O_2$ (IMP), (i) 10 wt.% Ni/CeO_2 (IMP), (j) 15 wt.% Ni/ZrO_2 (IMP), (k) 15 wt.% $Ni/Ce_{0.75}Zr_{0.25}O_2$ (IMP), (l) 15 wt.% Ni/CeO_2 (IMP).

As illustrated in Fig. 4, CH_4 conversion and CO selectivity at 700 °C are about 92 and 96%, respectively, over 5 wt.% Ni/CeO_2 and $Ni/Ce_{0.75}Zr_{0.25}O_2$ (IMP) catalysts. These values attained approach the equilibrium values as reported elsewhere [18]. In contrast, about 60% CH_4 conversion and 80% CO selectivity were achieved over 5 wt.% Ni/ZrO_2 (IMP) catalyst at the same reaction temperature. This indicates that 5 wt.% Ni/CeO_2 and $Ni/Ce_{0.75}Zr_{0.25}O_2$ (IMP) catalysts give higher MPO catalytic activity and selectivity to syngas than 5 wt.% Ni/ZrO_2.

With increasing Ni loading, the CH_4 conversion over Ni/CeO_2 and $Ni/Ce_{0.75}Zr_{0.25}O_2$ (IMP) catalysts was insignificantly increased (ca. 2%) whereas CO and H_2 selectivities were remained unchanged. For Ni/ZrO_2 (IMP) catalyst, the CH_4 conversion, CO and H_2 selectivities were considerably increased when increasing Ni loading from 5 to 10 wt.% but were insignificantly altered after which the Ni loading was increased to 15 wt.%. This may be due to the fact that CH_4 conversion, CO and H_2 selectivities approach the equilibrium values. At this point, the change in catalytic activity by catalyst would be less pronounced. Therefore, no effect could be observed as for the change in Ni loading.

The results indicated that the IMP catalysts are more active than GEL catalysts, as can also be seen in Fig. 4. It is believed that the decomposition of methane occurs on the metal [22]. The low activity of the catalysts prepared by gel impregnation method can be attributed to a lower degree of dispersion of metal compared to that of the catalysts prepared by impregnation method.

3.5. Coke formation

The CH_4/O_2 ratio also affects the catalytic activity of the catalysts. As given in Table 2, an increase in oxygen content in the feed stream ($CH_4/O_2 = 1.6$) resulted in decreasing CO and H_2 selectivities but remaining CH_4 conversion. In the case of insufficient oxygen ($CH_4/O_2 = 2.5$), the CH_4 conversion was found to decrease for 15 wt.% Ni/ZrO_2 (IMP) catalyst while it remained unchanged for 15 wt.% Ni/CeO_2 and 15 wt.% $Ni/Ce_{0.75}Zr_{0.25}O_2$ (IMP) catalysts. The CO and H_2 selectivities were slightly increased as an increase in CH_4/O_2 ratio. This might be due to the fact that CeO_2 and $Ce_{0.75}Zr_{0.25}O_2$ have considerable oxygen storage ability [16,25,26]. The evidence of coke formation was found at the CH_4/O_2 feed ratio of 2.5, indicating the H_2/CO ratio above 2.0 [12].

It was also observed that at a low Ni loading all catalysts are rather stable over a 24 h period of time on stream (data

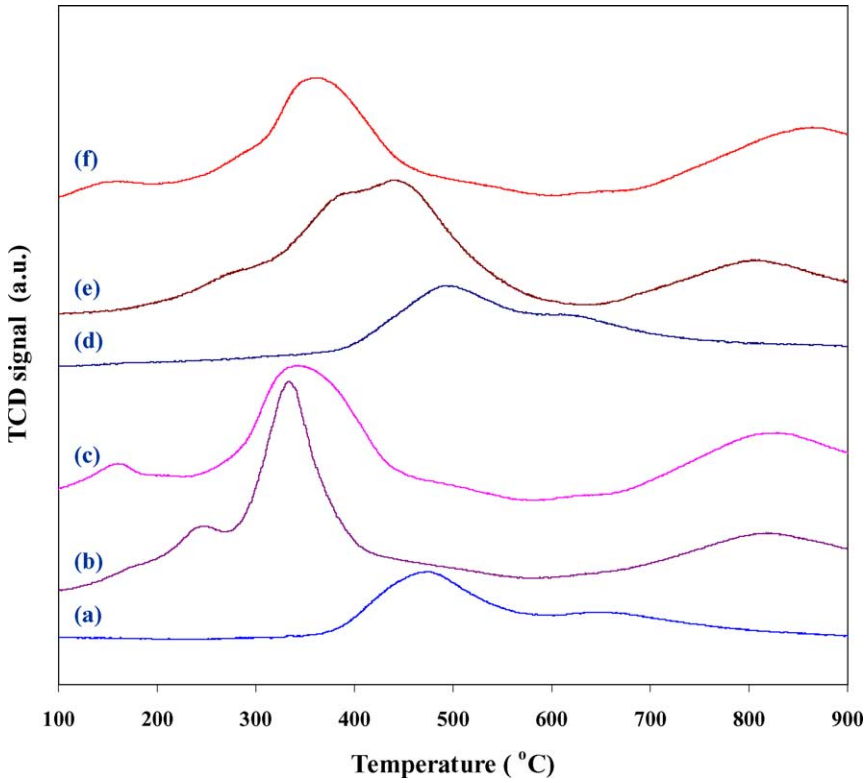

Fig. 3. H_2-TPR profiles of catalysts calcined at 500 °C with a heating rate of 10 °C min^{-1}, a reducing gas containing 5% hydrogen in nitrogen with a flow rate of 30 ml min^{-1}: (a) 5 wt.% Ni/ZrO_2 (IMP), (b) 5 wt.% $Ni/Ce_{0.75}Zr_{0.25}O_2$ (IMP), (c) 5 wt.% Ni/CeO_2 (IMP), (d) 5 wt.% Ni/ZrO_2 (GEL), (e) 5 wt.% $Ni/Ce_{0.75}Zr_{0.25}O_2$ (GEL), (f) 5 wt.% Ni/CeO_2 (GEL).

are not given). Thus, to compare the effect of support on coke formation, the high Ni loading of 15 wt.% was chosen. As can be seen from Fig. 5, the 15 wt.% Ni/ZrO_2 (IMP) catalyst possesses the least stability. However, the H_2/CO ratio of the catalysts is rather constant.

TPO technique was used to quantify the amount of carbon formed on the spent catalysts. The TPO profiles of 15 wt.% Ni/CeO_2 (IMP), 15 wt.% $Ni/Ce_{0.75}Zr_{0.25}O_2$ (IMP) and 15 wt.% Ni/ZrO_2 (IMP) catalysts (Fig. 6) show a large peak centered at ca. 650 °C for the formers and at ca. 700 °C for the latter, with an additional peak centered at the temperature of 550 °C. The two peaks observed on the TPO profile of 15 wt.% Ni/ZrO_2 (IMP) catalyst can be due to the presence of either different types of carbon or different sites of carbon deposited. The results are confirmed by TEM images as shown in Fig. 7. For spent Ni/CeO_2 and $Ni/Ce_{0.75}Zr_{0.25}O_2$ catalysts, it was observed that the only type of carbon deposition is in the form of filament. The carbon structure is graphitic with the usual constant spacing between layers. The dark particle in the end of tube would

Table 2
Methane partial oxidation on 0.1 g of 15% Ni/CeO_2 (IMP), 15% $Ni/Ce_{0.75}Zr_{0.25}O_2$ (IMP) or 15% Ni/ZrO_2 (IMP) catalysts using varied CH_4/O_2 feed at 100 ml/min flow rate (GHSV = 53,000 h^{-1})

Temperature (°C)	CH_4/O_2 feed ratio	15% Ni/CeO_2				15% $Ni/Ce_{0.75}Zr_{0.25}O_2$				15% Ni/ZrO_2			
		X_{CH_4} (%)	S_{CO} (%)	S_{H_2} (%)	H_2/CO	X_{CH_4} (%)	S_{CO} (%)	S_{H_2} (%)	H_2/CO	X_{CH_4} (%)	S_{CO} (%)	S_{H_2} (%)	H_2/CO
700	2.5	94	97	93	2.4	94	98	95	2.4	84	97	96	2.2
750	2.5	95	98	93	2.4	97	99	96	2.4	87	98	97	2.2
800	2.5	96	98	94	2.4	97	99	96	2.4	88	99	98	2.2
700	2.0	95	96	92	2.0	96	96	93	2.0	92	96	95	2.0
750	2.0	97	97	93	2.0	97	97	94	2.0	94	97	96	2.0
800	2.0	98	98	93	2.0	98	98	95	2.0	96	98	96	2.0
700	1.6	98	91	90	2.0	97	91	91	2.0	91	84	88	2.0
750	1.6	99	92	90	2.0	98	93	91	2.0	95	89	90	2.0
800	1.6	99	93	90	2.0	98	94	91	2.0	96	91	90	2.0

Note: the oxygen was completely consumed at all these cases.

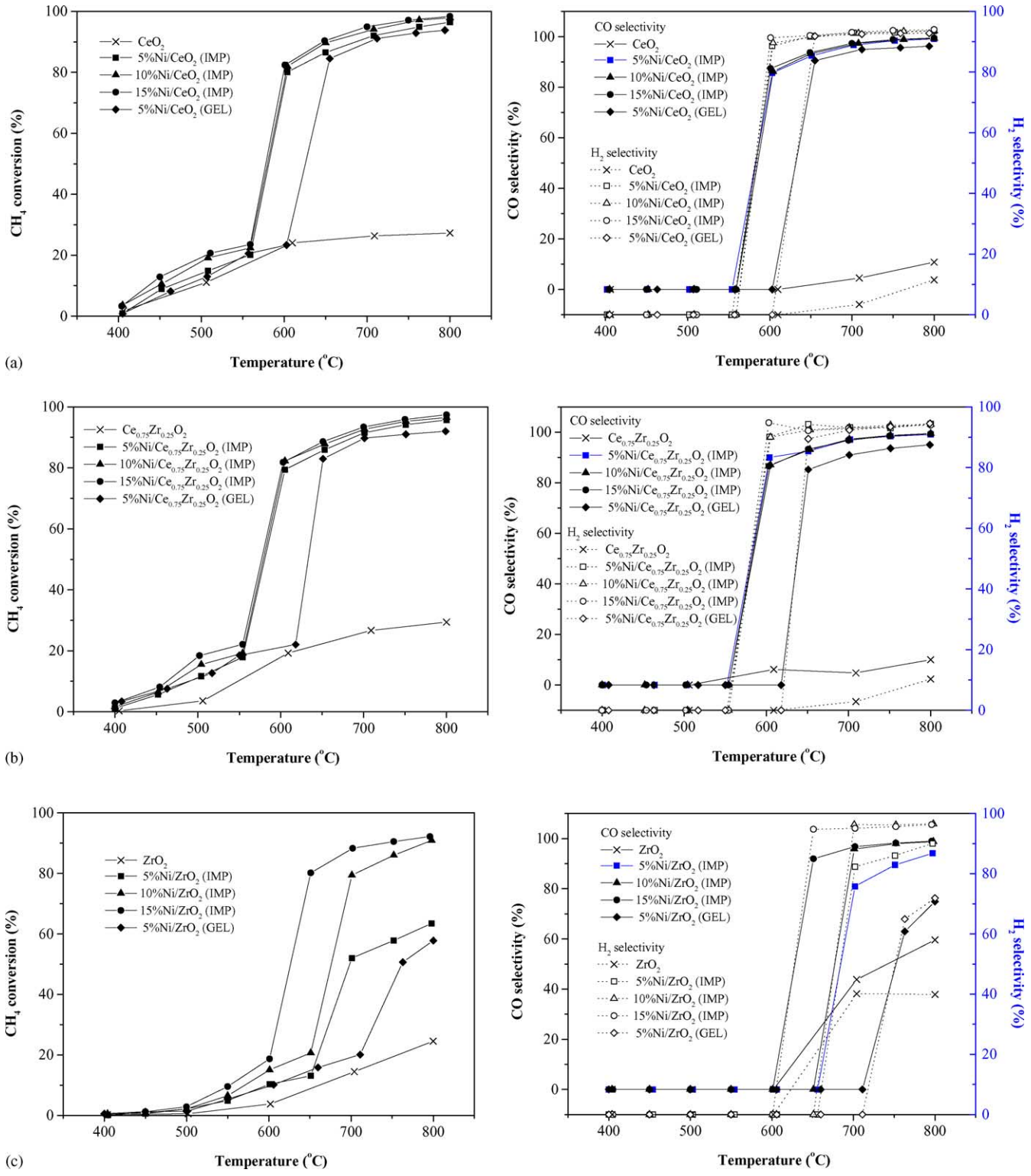

Fig. 4. The CH_4 conversion, CO selectivity and H_2 selectivity of methane partial oxidation over Ni-supported IMP catalysts calcined at 500 °C (CH_4/O_2 ratio of 2.0, GHSV = 106,000 h^{-1}): (a) Ni/CeO_2, (b) $Ni/Ce_{0.75}Zr_{0.25}O_2$, (c) Ni/ZrO_2.

be the encapsulated Ni species. For spent Ni/ZrO_2 catalyst, carbon nanotubes and graphite filaments were observed. The total amounts of carbon deposited on the spent catalysts are given in Table 3. The amount of carbon deposition was found in the order 15 wt.% $Ni/Ce_{0.75}Zr_{0.25}O_2$ (IMP) < 15 wt.% Ni/ZrO_2 (IMP) < 15 wt.% Ni/CeO_2 (IMP) indicating that $Ce_{0.75}Zr_{0.25}O_2$ can promote the oxidation of the carbon. This was also conformed by the CH_4-TPR experiments (Fig. 8), revealing that 15 wt.% $Ni/Ce_{0.75}Zr_{0.25}O_2$ catalyst can produce CO_2 more than can 15 wt.%

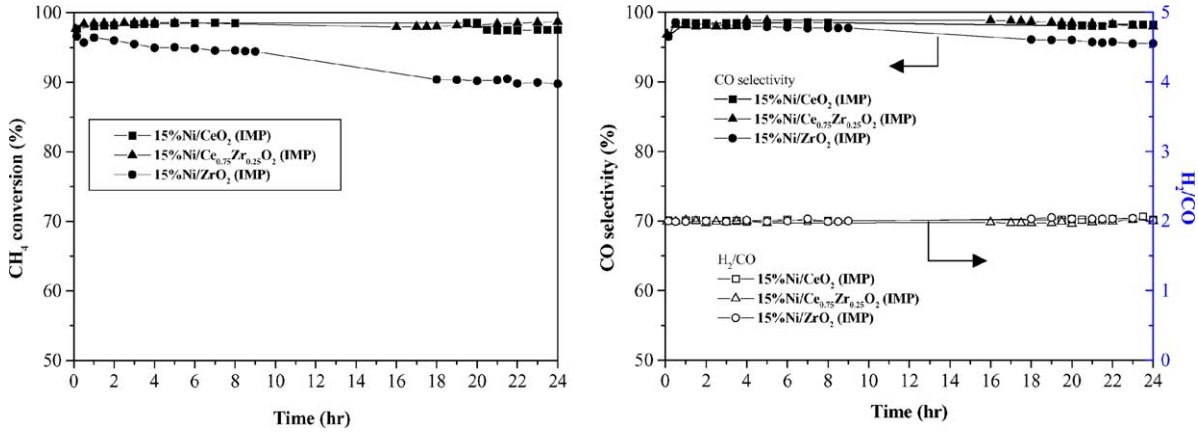

Fig. 5. The CH_4 conversion, CO selectivity and H_2/CO as a function of time over the IMP catalysts at 750 °C (CH_4/O_2 ratio of 2.0, GHSV = 53,000 h^{-1}).

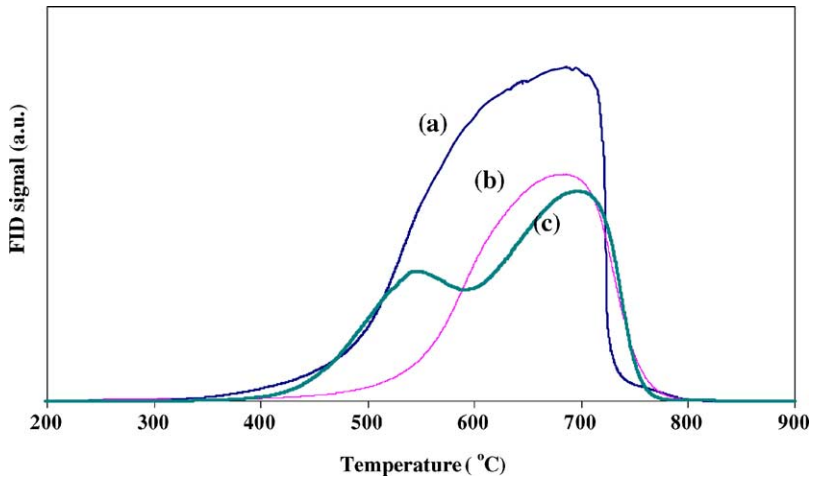

Fig. 6. TPO profiles of catalysts after exposure to reaction at 750 °C (CH_4/O_2 = 2.5, GHSV = 53,000 h^{-1}) for 4 h with a heating rate of 10 °C min^{-1}, an oxidizing gas containing 2% oxygen in He with a flow rate of 40 ml min^{-1}: (a) 15 wt.% Ni/CeO_2 (IMP), (b) 15 wt.% $Ni/Ce_{0.75}Zr_{0.25}O_2$ (IMP), (c) 15 wt.% Ni/ZrO_2 (IMP).

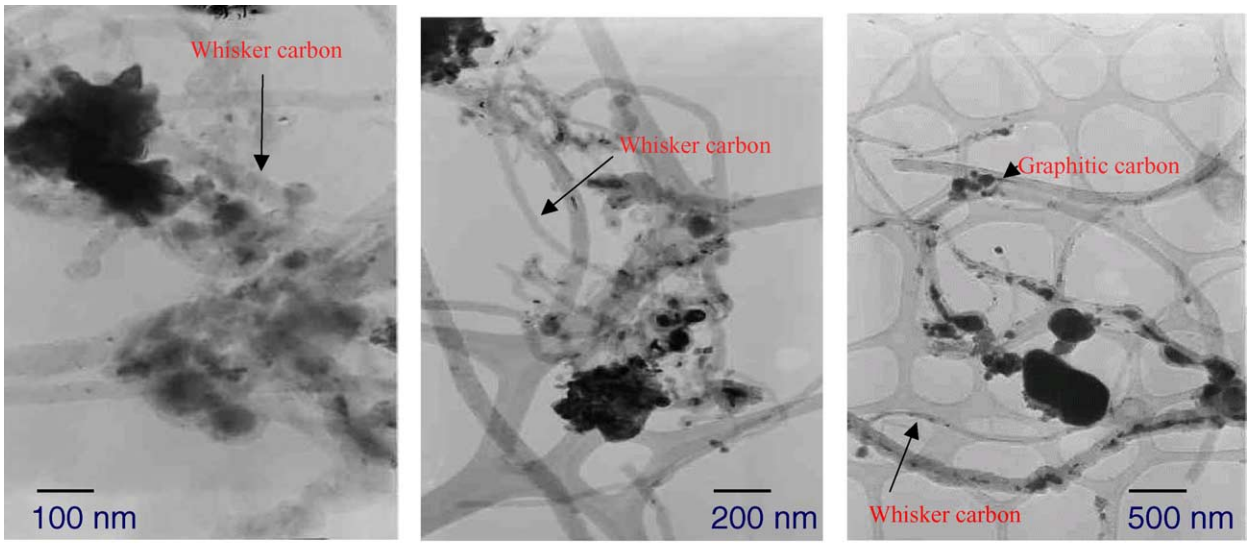

Fig. 7. TEM images of spent catalysts after exposure to reaction at 750 °C (CH_4/O_2 = 2.5, GHSV = 53,000 h^{-1}) for 4 h: (a) 15 wt.% Ni/CeO_2 (IMP), (b) 15 wt.% $Ni/Ce_{0.75}Zr_{0.25}O_2$ (IMP), (c) 15 wt.% Ni/ZrO_2 (IMP).

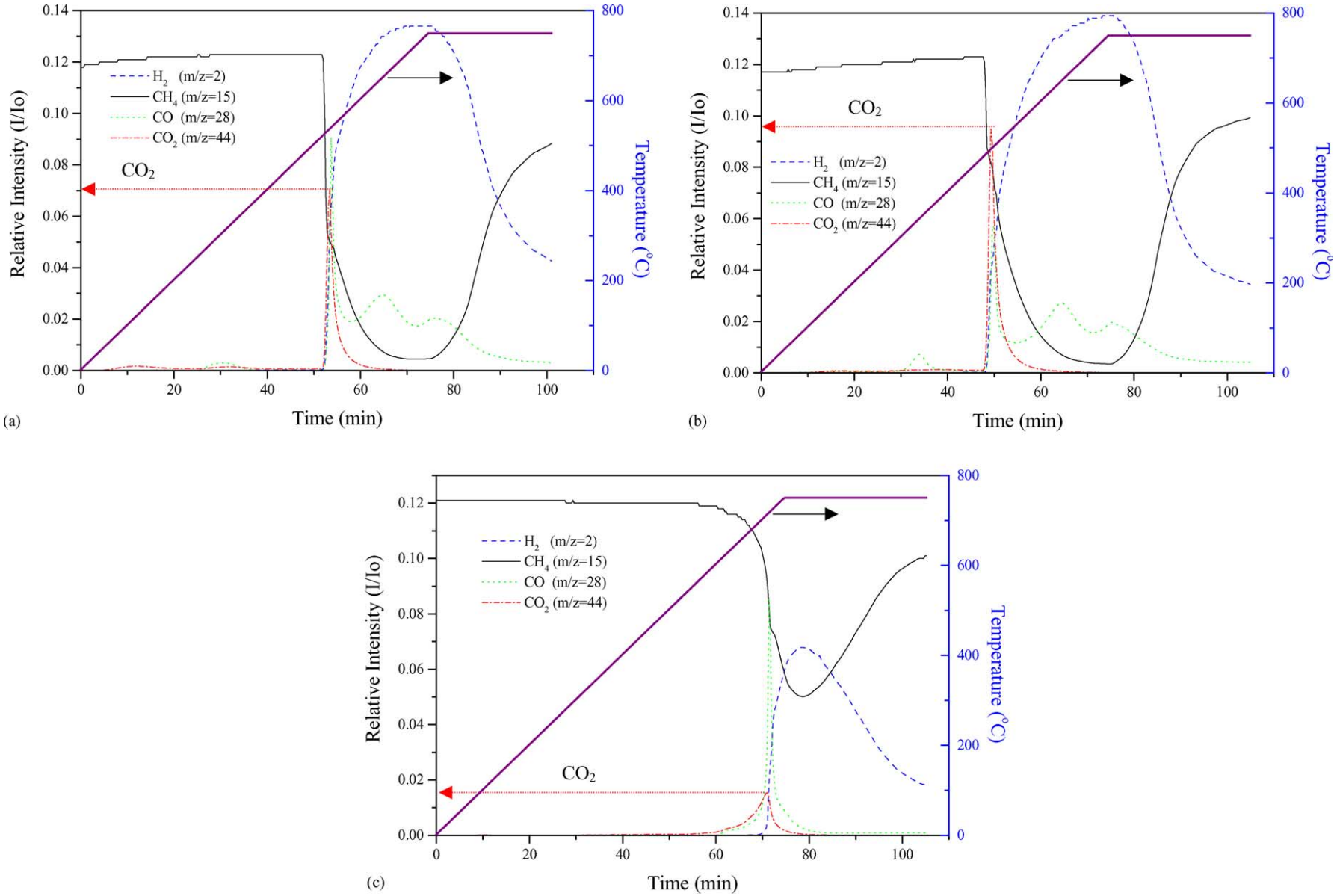

Fig. 8. CH_4-TPR profiles of catalysts calcined at 500 °C with a heating rate of 10 °C min^{-1} to 750 °C and held for 30 min, a reducing gas containing 2% CH_4 in He with a flow rate of 50 ml min^{-1}: (a) 15 wt.% Ni/CeO_2 (IMP), (b) 15 wt.% $Ni/Ce_{0.75}Zr_{0.25}O_2$ (IMP), (c) 15 wt.% Ni/ZrO_2 (IMP).

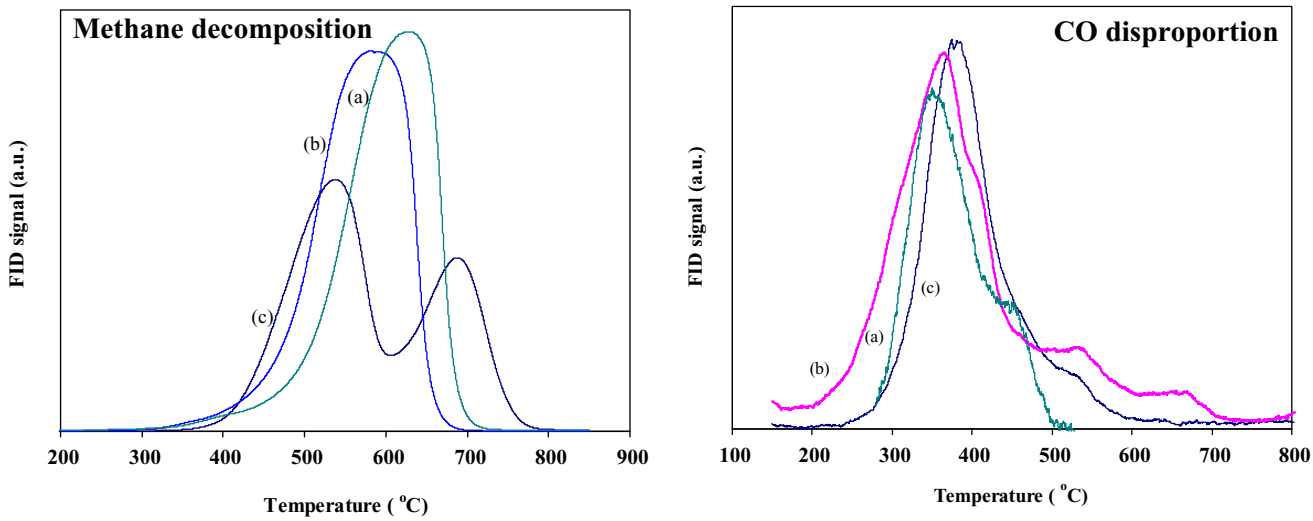

Fig. 9. TPO profiles of catalysts after exposure to reaction at 750 °C (2% CH_4 or 1% CO) for 1 h with a heating rate of 10 °C min^{-1}, an oxidizing gas containing 2% oxygen in He with a flow rate of 40 ml min^{-1}: (a) 15 wt.% Ni/CeO_2 (IMP), (b) 15 wt.% $Ni/Ce_{0.75}Zr_{0.25}O_2$ (IMP), (c) 15 wt.% Ni/ZrO_2 (IMP).

Ni/ZrO_2 and 15 wt.% Ni/CeO_2 catalysts. It is also concluded that 15 wt.% $Ni/Ce_{0.75}Zr_{0.25}O_2$ has a higher surface oxygen mobility [18].

The coke formation on these catalysts is due to the methane decomposition since the TPO profiles are rather analogous as shown in Fig. 9. The TPO profiles of methane decomposition over 15 wt.% Ni/CeO_2 (IMP), 15 wt.% $Ni/Ce_{0.75}Zr_{0.25}O_2$ (IMP) and 15 wt.% Ni/ZrO_2 (IMP) exhibit a large peak centered at ca. 600–700 °C with an additional peak centered at 550 °C for 15 wt.% Ni/ZrO_2

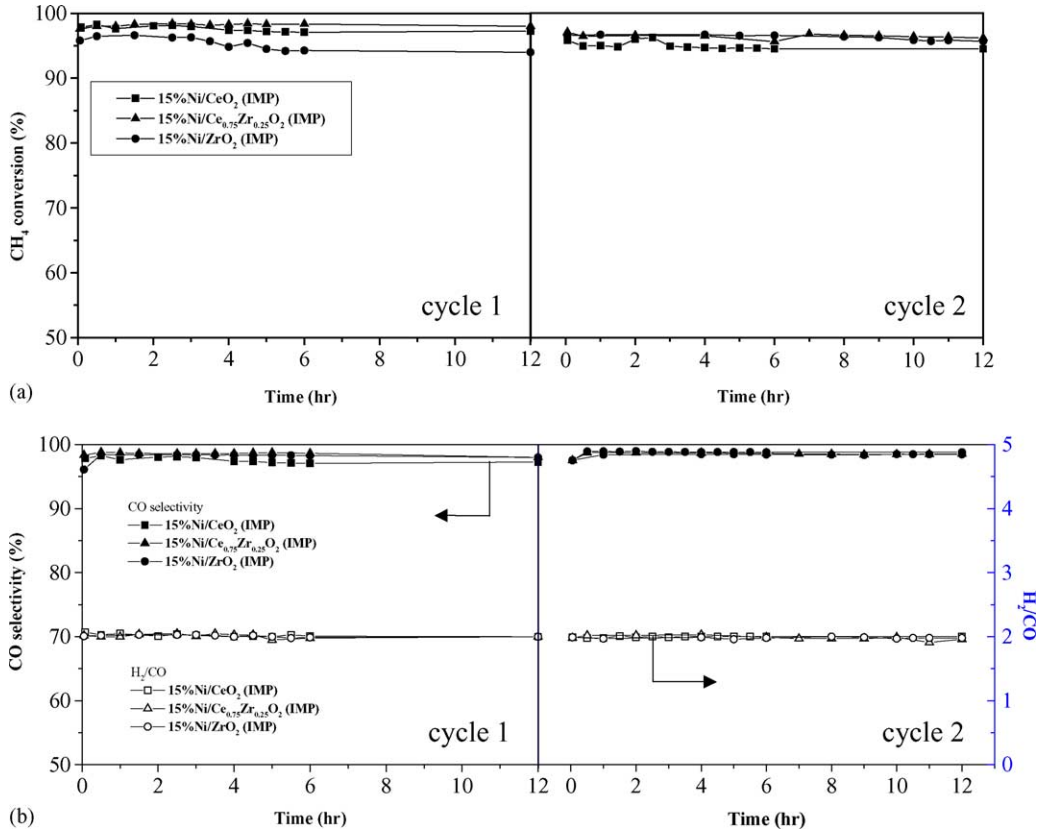

Fig. 10. The CH_4 conversion (a), CO selectivity and H_2/CO (b) as a function of time over the IMP catalysts at temperature of 750 °C (CH_4/O_2 ratio of 2.0, GHSV = 53,000 h^{-1}) compared with the regenerated catalysts with 21% O_2 in He at 500 °C.

Table 3
Amount of carbon deposition on the catalysts, as determined by TPO, using 2% O_2 in He and heating rate of 10 °C min^{-1}, after 4 h reaction at 750 °C and CH_4:O_2 ratio of 2.5

Catalyst	CH_4 conversion[a] (%)	CO selectivity (%)	H_2 selectivity (%)	Percent of carbon (wt.%)
15% Ni/CeO_2 (IMP)	95	98	93	22.70
15% $Ni/Ce_{0.75}Zr_{0.25}O_2$ (IMP)	97	99	96	12.87
15% Ni/ZrO_2 (IMP)	87	98	97	15.82

[a] Conversion at the end of reaction time (4 h).

(IMP) catalyst. On the contrary, the TPO profiles of CO disproportion over 15 wt.% Ni/CeO_2 (IMP), 15 wt.% $Ni/Ce_{0.75}Zr_{0.25}O_2$ (IMP) and 15 wt.% Ni/ZrO_2 (IMP) exhibit a peak centered at ca. 300–400 °C.

It should be noted that after the regeneration under 21% O_2 balanced with He at 500 °C for 1 h, the original activity and selectivity were regained as shown in Fig. 10. The H_2/CO ratio of 2.0 ± 0.05 was still obtained for these regenerated catalysts.

4. Conclusions

It can be concluded that the catalysts prepared by impregnation method showed higher catalytic activity for methane partial oxidation than those prepared by gel impregnation method due to a better metallic Ni dispersion and reducibility. The Ni/CeO_2 and $Ni/Ce_{0.75}Zr_{0.25}O_2$ catalysts showed higher catalytic activity for methane partial oxidation than Ni/ZrO_2 catalyst. The H_2/CO molar ratio of 2.0 was achieved at a CH_4/O_2 ratio of 2.0 for all catalysts. The effect of CH_4/O_2 ratio on the activity and H_2/CO was more pronounced with Ni/ZrO_2 than Ni/CeO_2 and $Ni/Ce_{0.75}Zr_{0.25}O_2$ catalysts. The CH_4 conversion slightly increased while CO and H_2 selectivities remained unchanged with increasing Ni loading for Ni/CeO_2 and $Ni/Ce_{0.75}Zr_{0.25}O_2$ catalysts. The $Ni/Ce_{0.75}Zr_{0.25}O_2$ catalyst showed the highest stability with a little carbon deposition after prolonged reaction time. The carbon on the surface of the catalyst was due mainly to the methane decomposition. The original activity and selectivity can be retrieved by oxidizing the spent catalysts with oxygen.

Acknowledgements

The authors would like to thank RGJ, Ph.D. program, Thailand Research Fund and Ratchadapiseksomphote Fund, CU for the financial support. We acknowledged Dr. Toranin Chairuangsri of Electron Microscope Centre, Chaingmai University for his assistance on TEM analysis.

References

[1] D. Dissanayake, M.P. Rosynek, K.C.C. Kharas, J.H. Lunsford, J. Catal. 132 (1991) 177.
[2] Y. Lu, J. Xue, C. Yu, Y. Liu, S. Shen, Appl. Catal. A 174 (1998) 121.
[3] S.A. Chellappa, S.D. Viswanath, Ind. Eng. Chem. Res. 34 (1995) 1933.
[4] C.T. Au, H.Y. Wang, H.L. Wan, J. Catal. 158 (1996) 343.
[5] Y.H. Hu, E. Ruckenstein, J. Catal. 158 (1996) 260.
[6] Y. Boucouvalas, Z. Zhang, X.E. Verykios, Catal. Lett. 27 (1994) 131.
[7] Y. Boucouvalas, Z. Zhang, X.E. Verykios, Catal. Lett. 40 (1996) 189.
[8] D.A. Hickman, L.D. Schmidt, Science 259 (1993) 343.
[9] E.P.J. Mallens, J.H.B.J. Hoebink, G.B. Marin, J. Catal. 167 (1997) 43.
[10] K. Otsuka, Y. Wang, M. Nakamura, Appl. Catal. A 183 (1999) 317.
[11] P. Pantu, K. Kim, G.R. Gavalas, Appl. Catal. A 193 (2000) 203.
[12] P. Pantu, G.R. Gavalas, Appl. Catal. A 223 (2002) 253.
[13] S.J. Hargreaves, J.H. Graham, J.W. Richard, Lett. Nat. 348 (1990) 428.
[14] B. Irigoyen, N. Castellani, A. Juan, J. Mol. Catal. A 129 (1998) 297.
[15] E. Ruckenstein, H.Y. Hu, Appl. Catal. A 183 (1999) 85.
[16] K. Otsuka, Y. Wang, E. Sunada, I. Yamanaka, J. Catal. 175 (1998) 152.
[17] J.A. Montoya, E. Romero-Pascual, C. Gimon, P. Del Angle, A. Monzon, Catal. Today 63 (2000) 71.
[18] T. Zhu, M. Flytzani-Stephanopoulos, Appl. Catal. A 208 (2001) 403.
[19] Q. Miao, G. Xiong, S. Sheng, W. Cui, L. Xu, X. Guo, Appl. Catal. A 154 (1997) 17.
[20] S. Tang, J. Lin, K.L. Tan, Catal. Lett. 51 (1998) 169.
[21] H.M. Swann, V.C.H. Kroll, G.A. Martin, C. Mirodatos, Catal. Today 21 (1994) 571.
[22] F.B. Noronha, E.C. Fendley, R.R. Soares, W.E. Alvarez, D.E. Resasco, Chem. Eng. J. 82 (2001) 21.
[23] S.M. Stagg-Williams, F.B. Noranha, G. Fendley, D.E. Resasco, J. Catal. 194 (2000) 240.
[24] W. Dong, K. Jun, H. Roh, Z. Liu, S. Park, Catal. Lett. 78 (2002) 215.
[25] P. Fornasiero, D.R. Monte, G.R. Ranga, J. Kaspar, S. Meriani, A. Trovarelli, M. Graziani, J. Catal. 151 (1995) 168.
[26] P. Fornasiero, G. Balducci, R.D. Monte, J. Kaspar, V. Sergo, G. Gubitosa, A. Ferrero, M. Graziani, J. Catal. 164 (1996) 173.
[27] J.R. Gonzalez-Velasco, A.M. Gutierrez-Ortiz, M. Jean-Louis, A.J. Botas, P.M. Gonzalez-Marcos, G. Blanchard, Appl. Catal. B 22 (1999) 167.
[28] E.C. Hori, H. Permana, K.Y. Simon, A. Brenner, K. More, M.K. Rahmoeller, D. Belton, Appl. Catal. B 16 (1998) 105.
[29] H. Roh, K. Jun, W. Dong, J. Chang, S. Park, Y. Joe, J. Mol. Catal. A 181 (2002) 137.
[30] S. Pengpanich, V. Meeyoo, T. Rirksomboon, K. Bunyakiat, Appl. Catal. A 234 (2002) 221.
[31] T. Takeguchi, S. Furukawa, M. Inoue, J. Catal. 202 (2001) 14.
[32] T. Shishido, M. Sokenobu, H. Morioka, M. Kondo, Y. Wang, K. Takaki, K. Takehira, Appl. Catal. A. 223 (2002) 235.